

Dendrimer-Based Nanomedicine

A nanoscopic multivalent antigen-presenting carrier for sensitive detection and drug delivery to T Cells

Tarek M. Fahmy, PhD,^{a,*} Jonathan P. Schneck, PhD,^b W. Mark Saltzman, PhD^a

^aDepartment of Biomedical Engineering, Yale University, New Haven, Connecticut, USA

^bDepartment of Pathology, Johns Hopkins School of Medicine, Baltimore, Maryland, USA

Received 18 August 2006; accepted 21 November 2006

Abstract

Both monoclonal T cell-specific antibodies and multivalent major histocompatibility complex proteins are used as diagnostic reagents for T cell-mediated diseases. However, their widespread use as vehicles for drug delivery has been hindered by the lack of versatile methods that couple the targeting potential of these reagents with drugs of clinical relevance. To address this problem, we engineered a multivalent nanoscopic drug carrier that flexibly tethers to a variety of T-cell antigens. Our carriers bound their target T cells specifically and with enhanced sensitivities as compared with free antigen. Additionally, they consistently inhibited the proliferation of the target T cells in vitro and in vivo, whereas drug-free constructs elicited strong stimulation of the target populations. As a result of the flexibility of incorporating multivalent antigen and drug, these carriers have wide potential use as sensitive T-cell detection reagents as well as promising immunostimulatory or immunosuppressive tools.

© 2007 Elsevier Inc. All rights reserved.

Key words:

Peptide-loaded major histocompatibility complex; T-cell receptor; Polyethylene glycol; Polyamidoamine dendrimer; Streptavidin

T cells and their antigen-specific subsets are important for the maintenance of a normal immune response, and aberrant function of those cells contributes to the pathogenesis of many chronic autoimmune and alloimmune disease states. Although the ability to detect T cells and antigen-specific T cells in vitro and in vivo would be helpful for disease diagnosis [1,2], the added ability to modulate these cells would lead to novel approaches for repairing immune system defects and restoring immune competence. One approach for modulating the antigen-specific response involves the induction of antigen-specific T-cell unresponsiveness or anergy by exposure to controlled doses of antibodies or peptide–major histocompatibility complex ligands (peptide-MHC). This approach has traditionally

required multiple treatments and has limitations because affected T cells remain alive in a hyporesponsive state that could be reversed by a variety of factors, including the presence of certain cytokines or the absence of antigen [3]. A second approach involves the conjugation of T cell antigens to immunosuppressive drugs, which would serve to direct drug delivery to a targeted population of T cells [4]. However, conjugation of drug to carrier antigens requires chemical modifications that are not always easy to achieve. In addition, the effectiveness of conjugates is often limited, because it is difficult to provide unhindered antigen presentation together with effective drug delivery.

Targeting of antigen-specific T cells is further complicated by the intrinsic low affinity of peptide-MHC to T cell receptor (TCR) binding, which is in the range of 1 to 100 μM [5,6]. Multivalency can be used to enhance interactions via avidity: for example, doubling the valency of peptide-MHC complexes can substantially lower the dissociation constant [7]. Therefore, we sought to engineer multivalent T cell

No conflict of interest was reported by the authors of this paper.

* Corresponding author. Malone Engineering Center, Yale University, New Haven, CT 06511.

E-mail address: tarekfahmy@yale.edu (T.M. Fahmy).

targeting for enhanced avidity and sensitive detection of specific T cells. In addition, if such constructs could be endowed with the ability to load drug molecules, they would be attractive reagents for sustaining the interactions necessary for drug delivery to their target T cells.

To accomplish these goals, we engineered a robust, antigen-presenting carrier by linking bifunctional poly(ethylene glycol) (PEG) chains to a “nanocarrier”, poly(amidoamine) spherical core (PAMAM), which functions as a drug carrier. We encapsulated doxorubicin (Dox), a potent antimetabolic drug, into the PAMAM core (32 mol Dox per mole construct), and the surface of the carrier was modified with antibodies or MHC molecules. This surface modification facilitated high-avidity interactions for detection of target T cells and also allowed for specific drug delivery through receptor-mediated internalization of the complexes. The activity of these complexes, according to both *in vitro* and *in vivo* experiments, suggests their promise as sensitive reagents for both detection and drug delivery to different populations of T cells.

Materials and methods

Mice

All animals were routinely used at 6 to 8 weeks of age and were maintained under specific pathogen-free conditions and routinely checked by the Yale University Animal Resource Center. BALB/c mice were obtained from Jackson Laboratories (Bar Harbor, ME). 2C TCR transgenic mice breeding pairs were a gift from Dr. Fadi Lakkis (Yale University School of Medicine). 2C mice were maintained as heterozygous by breeding on a C57BL6 background in our animal facility. Phenotypes were tested with the clonotypic 1B2 antibody.

Cells

All cells used were obtained from homogenized naive mouse spleens after depletion of red blood cells by hypotonic lysis. CD3⁺ and CD8⁺ cells were isolated by negative selection from 2C splenocytes using CD3 T cell or CD8⁺ T-cell subset enrichment columns (R&D Systems, Minneapolis, MN). Purity greater than 95% was routinely obtained.

PEG-PAMAM

PAMAM Generation 6 (Aldrich, Milwaukee, WI), 10 wt% in methanol, was evaporated under a gentle stream of nitrogen and placed under high vacuum overnight before further manipulation. To prepare fluorescently labeled constructs, a 24-fold molar excess of Boc-NH-PEG3400-NHS COOH and a 6-fold molar excess of fluorescein-PEG5000-NHS COOH (Nektar Pharmaceuticals, Huntsville AL) were added to PAMAM in a 0.2 M borate buffer pH 8.0. For unlabeled constructs a 30-fold molar excess of PEG3400 was used. The mixture was vortexed gently and placed on a rotary shaker for 24 hours. Unreacted PEG was

removed by dialysis in a 10,000 MWCO Slide-a-Lyser (Pierce, Rockford, IL) with borate as the dialysis buffer. To remove the tBoc protecting group, the complex was lyophilized for 48 hours and redissolved in trifluoroacetic acid for 30 minutes at room temperature (23°C–25°C) with constant stirring. Trifluoroacetic acid was removed under vacuum for 1 hour. The remaining product was dissolved in borate buffer followed by dialysis in water. The final PEG-PAMAM complex was lyophilized once more and stored at –20°C. The characterization of these complexes is discussed in detail in a previous report [8].

Streptavidin-PEG-PAMAM

Streptavidin (Sigma, St. Louis, MO) was activated for amine coupling by dissolving at 1 mg/mL in 0.1 M methyl ethane sulfonate, 0.5 M NaCl buffer pH 5.1. To form active ester functional groups for coupling, NHS (*N*-hydroxysuccinimide) and EDC (1-ethyl-3-[3-dimethylaminopropyl]carbodiimide HCl), both from Pierce (Rockford, IL) were added at a concentration of 5 mM and 2 mM, respectively, and allowed to react for 15 minutes at room temperature. The unreacted EDC was quenched with 2-mercaptoethanol at a final concentration of 20 mM. For amine coupling to the PEG-PAMAM, a 20-fold molar excess of activated streptavidin was added to the PEG-PAMAM and reacted for 2 hours at room temperature. Excess reactant and unconjugated streptavidin was removed by extensive dialysis in a 300K MWCO CE ester membrane (Spectrum Laboratories, Rancho Dominguez, CA). Homogeneity of the complexes was assessed by reverse-phase high-performance liquid chromatography (HPLC) on a C18 column (Supelco) with 30% acetonitrile in 1× phosphate-buffered saline (PBS) as the mobile phase.

Dynamic light scattering

The size of the constructs were measured by dynamic light scattering. The instrument consisted of a diode-pumped laser (Verdi V-2/V-5, Coherent) operating at 532 nm, an ALV-SP S/N 30 goniometer (ALV-GmbH, Langen, Germany) with index matching vat filled with doubly filtered (0.1 mM) toluene, and an ALV-500 correlator. Low concentrations of constructs (<5 μg/mL) were pipetted into a cleaned borosilicate culture tube before measuring the intensity of the autocorrelation function at a 90-degree scattering angle. The hydrodynamic radius (*R_H*) was determined by nonlinear least squares fitting (ALV software) of the resulting second-order cumulants.

Antibody and MHC coupling

Biotinylated antibodies (biotin-conjugated hamster anti-mouse CD3ε and biotin-conjugated rat anti-mouse CD45R/B220) (BD Biosciences, PharMingen, San Jose, CA) were used without further purification. Soluble MHC-immunoglobulin (MHC-Ig) dimers K^b-Ig and L^d-Ig were prepared by methods described previously [9]. MHC monomers were

prepared from the same dimer stock used in binding experiments by papain treatment of the MHC-Ig and purified as recommended by the manufacturer (Pierce Immunopure Fab preparation kit; Pierce, Rockford, IL). Preparation of MHC-Ig Fab fragments by papain treatment yielded functionally active protein that specifically bound 2C TCR immobilized to the surface of a biosensor (Biacore, Piscataway, NJ) (data not shown). MHC L^d monomers and dimer were fluorescently labeled with fluorescein isothiocyanate (FITC; Molecular Probes, Carlsbad, CA) at pH 7.4 and purified by size exclusion chromatography. Protein concentrations were determined spectrophotometrically by measuring the absorbance at 280 nm. Biotinylated antibodies or MHC monomers were added at the molar ratio of 40:1 to streptavidin-coupled PEG-PAMAM and incubated overnight at 4°C followed by dialysis in a 300K MWCO CE membrane (Spectrum Laboratories, Rancho Dominguez, CA). Both K^b and L^d constructs and K^b dimers were loaded with peptide and refolded in the presence of 40-fold molar excess peptide and 2-fold molar excess β₂-microglobulin according to methods described previously [7,10]. Peptides were synthesized by the Yale University Biotechnology Resource Laboratory, purified by HPLC, and purity tested by mass spectroscopy. Using a conformationally sensitive enzyme-linked immunosorbent assay, we have estimated that more than 85% of the K^b and L^d constructs were folded properly on the construct (data not shown).

Dox loading of PEG-PAMAM constructs

Dox was dissolved in water at a final concentration of 2.5 mg/mL and added to a final concentration of 100 nM to PEG-PAMAM constructs in PBS pH 7.4. The solution was mixed gently for 2 hours at 37°C then 24 hours at 4°C, followed by dialysis in 7000 MWCO membranes (Pierce, Rockford, IL). Encapsulation efficiency was assessed by fluorescence emission at 570 nm with 488 nm excitation. The amount of Dox loaded was deduced from a Dox calibration standard. To assess the magnitude of Dox fluorescence enhancement in the presence of PEG-PAMAM constructs, Dox at 2.5 mg/mL in water was titrated in 0.1-μL volumes in a fluorometer cuvette in the presence or absence of PEG-PAMAM constructs. Difference spectra were collected in the range 500 to 600 nm with excitation at 488 nm.

T-cell binding assay

Cells (1×10⁵) were incubated with varying concentrations of the reagents, until equilibrium binding was achieved (2 hours, 4°C). Cells were washed three times with 1×PBS containing 1% fetal calf serum (FCS) and 0.1% sodium azide and analyzed by flow cytometry on a FACScan (BD Biosciences). The mean channel fluorescence (MCF) was a measure of the amount of reagent bound, and the fraction bound at any specific concentration was deduced by dividing the MCF by the maximum MCF of the binding reagent in the experiment.

In vitro T-cell proliferation assays

Cells were adjusted to a concentration of 1×10⁷ cells/mL in complete medium. Plates were coated with various concentrations of anti-CD3ε antibodies according to established protocols [11]. Per well, 2×10⁵ cells were plated. Cells were treated with 20 nM complexes either loaded or not loaded with Dox and incubated at 37°C, 5% CO₂. On day 3 T-cell proliferation was analyzed with a colorimetric assay for quantification of cell proliferation and viability, WST-1, according to the manufacturer's protocol (Roche Diagnostics GmbH, Penzance, Germany). Degree of proliferation of treated cells (experimental) was quantitated by comparing to untreated cells (control) according to the formula: proliferation index = [(1 - (control - experimental)/control)].

Data fitting

We fitted our in vitro proliferation data to a dose-response logistic function using Microcal origin 6.0:

$$\text{Proliferation} = 1 - \frac{\text{Control} - \text{Experimental}}{\text{Control}}$$

$$= \frac{A_1 - A_2}{1 + \left(\frac{[\text{DOX}]}{X_{50}}\right)^P} + A_2$$

Here A_1 and A_2 represent the initial and final proliferation index values, P is the slope of the dose-response curve, and X_{50} is the dose for half-maximal proliferation.

Stimulation and inhibition of T cells in vivo

The experimental protocol consisted of injecting mice with 1 × 10⁷ purified 2C CD8⁺ T cells in 100 μL of sterile PBS. One day after adoptive transfer, mice were injected intraperitoneally with 200 μg of constructs, either drug-free or carrying 3.6 μg of Dox. This is well below the LD₅₀ of 21 μg/g of body weight for intravenous administration of Dox to mice. Four days after this treatment 1×10⁶ splenocytes were isolated and stained for the frequency of 2C cells by analysis with the clonotypic antibody against the 2C TCR, 1B2.

Results

Engineering high-avidity antigen presentation

Our strategy for constructing T-cell binding reagents is shown in Figure 1, A. The reagents are built from a hydrophobic dendrimer core (6.7 nm) with radiating PEG chains (4.2 nm) terminated with functional amines, which were coupled to streptavidin. This construct was assembled to contain multiple (24–30) PEG chains and generation 6 PAMAM [12] using methods reported previously [8]. Briefly, the condensation reaction of PAMAM and activated ester tBOC-NH-PEG-3400-COOH (molar ratio of 1:30), was carried out in borate buffer at pH 8.0. In experiments that used fluorescent conjugates this reaction was also

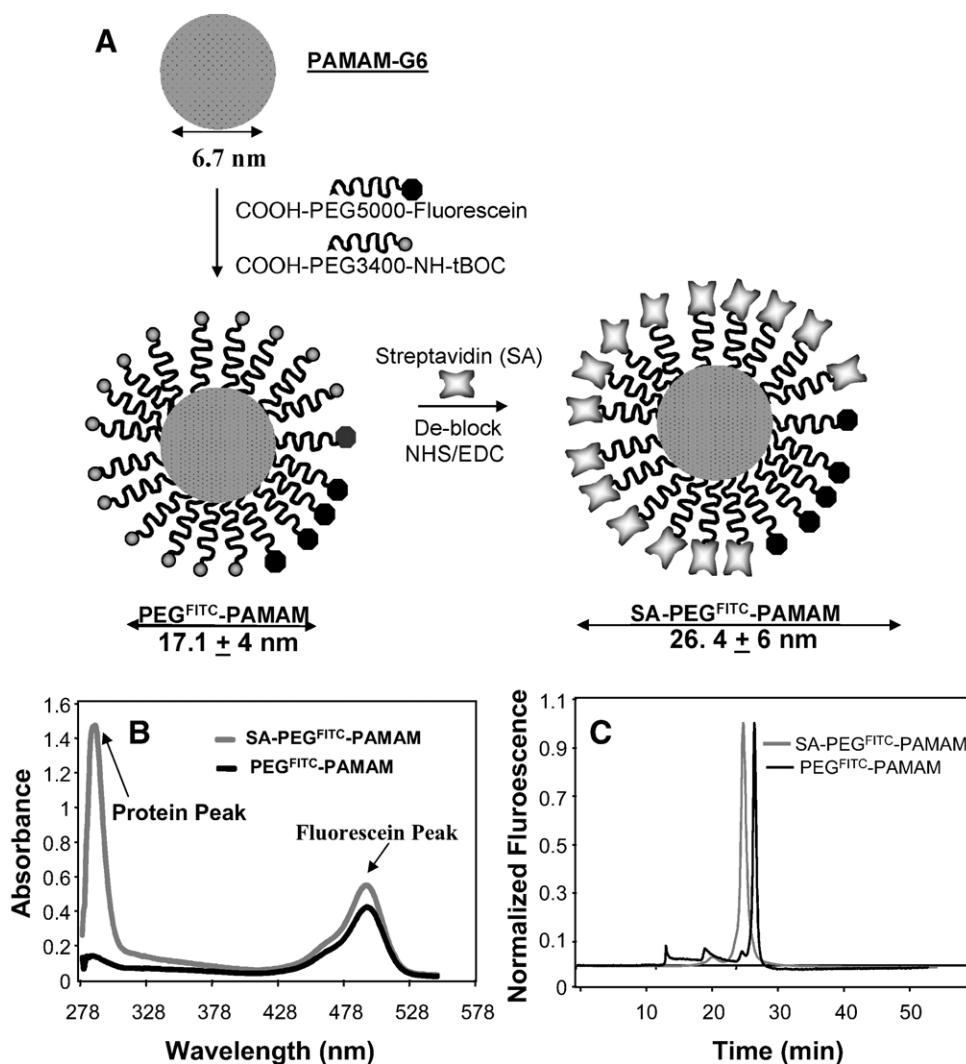


Fig 1. Schematic representation of SA-PEG^{FITC}/PAMAM construction. **A**, The construction of streptavidin-PEG^{FITC}/PAMAM is described in detail in the Methods section. **B**, Absorbance profiles of streptavidin-PEG^{FITC}/PAMAM and PEG^{FITC}/PAMAM. The level of streptavidin conjugation was deduced from standards and is equivalent to 13 mol of streptavidin per mole of construct. **C**, Reverse-phase HPLC of SA-PEG^{FITC}/PAMAM and PEG^{FITC}/PAMAM. Mobile phase is 30% acetonitrile in PBS. Stationary phase is a C18 column.

carried out with HOOC-PEG5000-fluorescein (molar ratio of 1:25:5, PAMAM/HOOC-PEG3400-NH-tBoc/HOOC-PEG5000-fluorescein, respectively). Characterization of the conjugate was performed with Fourier transform infrared (FT-IR). FT-IR spectra showed the appearance of an amide bond at (1672 cm^{-1}), confirming the formation of the conjugates and a peak at (1720 cm^{-1}), corresponding to the presence of tBoc ester.

We chose PAMAM dendrimers for two reasons. First, the PAMAM cores can function as vehicles for small drugs [13–15], paramagnetic molecules for contrast enhancement in magnetic resonance imaging [16], oligonucleotides [8], transgenes [17,18], and radionuclides [19]. Second, because of their branched tree-like structure, PAMAM tendrils radiate out from a central hydrophobic core to create a well-defined globular architecture with 256 functional amine groups at the surface [20]. This facilitated the

attachment of a high density of a variety of ligands. We attached fluorochrome-terminated PEG chains (MW 5000) and amine-terminated PEG (MW 3400) at the molar ratio of 1:5. Streptavidin was coupled to amine-terminated PEG chains by NHS-EDC chemistry with an efficiency of 13 streptavidin molecules per construct (Figure 1, B). Reverse-phase HPLC of the constructs (Figure 1, C) revealed a narrow distribution of the PEG-PAMAM and a slightly wider distribution for streptavidin-PEG-PAMAM (SA-PEG-PAMAM) constructs. The SA-PEG-PAMAM eluted earlier on a C18 column, probably as a result of the decrease in hydrophobicity of the construct that occurred with streptavidin conjugation. Construct size was determined by dynamic light scattering and estimated at 17.1 nm and 26.4 nm for PEG-PAMAM and SA-PEG-PAMAM, respectively. In summary, chemical analysis of our constructs is consistent with the model depicted in Figure 1, A.

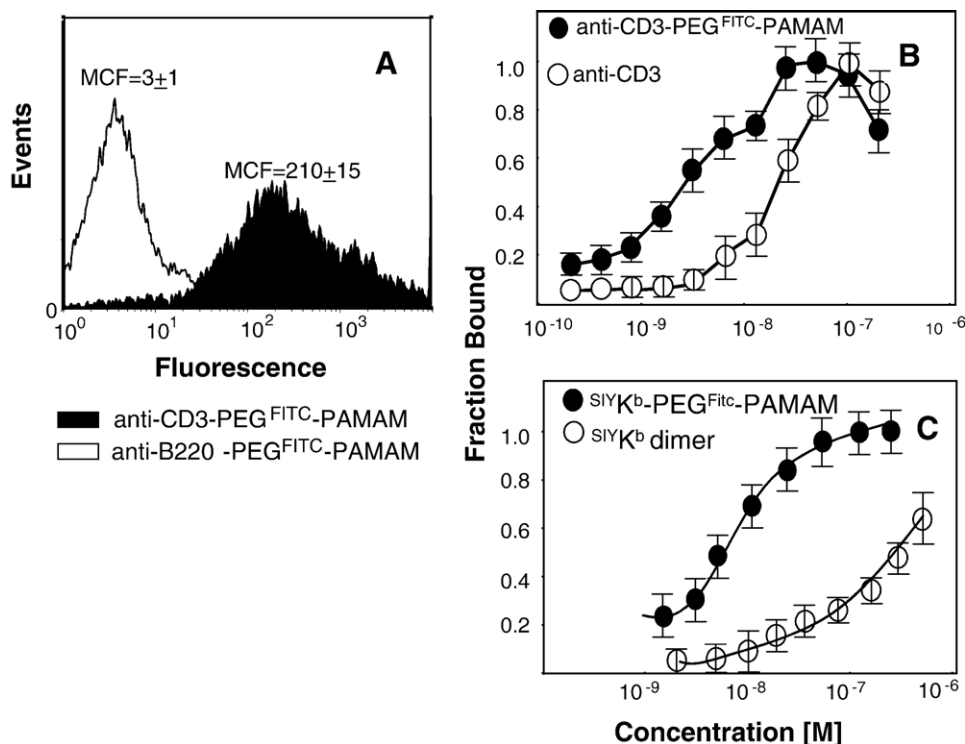


Fig 2. Antigen-presenting constructs bind T cells with specificity and high avidity. **A**, Purified CD3⁺ T cells isolated from BALB/c splenocytes by negative selection (1×10^5) were incubated with 20 nM of anti-CD3e or anti-CD45R/B220 (negative control that recognizes B cells) fluorescein-labeled constructs at 4°C for 2 hours. The cells were washed three times with PBS containing 2% FCS and 0.1% sodium azide, and analyzed for bound fluorescence by flow cytometry. **B**, Direct flow cytometry binding assay. Purified T cells from BALB/c mice (1×10^5) were incubated with various concentrations of anti-CD3 SA-PEG^{FITC}/PAMAM constructs or anti-CD3-FITC for 2 hours at 4°C. **C**, Purified 2C CD8⁺ T cells (1×10^5) isolated from 2C transgenic splenocytes by negative selection were incubated with various concentrations of ^{SIYK^b}-SA-PEG^{FITC}/PAMAM or ^{SIYK^b}-Ig FITC (MHC dimer). Specific concentrations (x-axis) are that of the MHC. In both **B** and **C**, cells were washed three times with PBS–2% FCS and 0.1% sodium azide, then analyzed by flow cytometry (see Methods section). The amount of bound reagent is determined from the mean channel fluorescence (MCF). Normalized fluorescence (fraction bound) is the MCF divided by the maximum MCF in the experiment. Experiments were performed in triplicate; shown are the mean and standard deviation (error bars). The experiment shown is a representation of one of at least three independent studies with similar results.

Antigen-presenting constructs bind their targets with specificity and high avidity

To evaluate the specificity of SA-PEG-PAMAM as a multivalent scaffold for T-cell ligands, we coupled SA-PEG-PAMAM to biotinylated antibodies that recognize either the T-cell CD3 complex or the CD45R (B220) antigen on B cells (negative control). In T-cell populations, virtually no binding of the control anti-B220 complexes was seen at the saturating doses used in this study, but the specific anti-CD3 complex bound strongly at the same dose (Figure 2, A). When the anti-CD3 complexes were incubated at various concentrations with T cells, we noticed a striking enhancement in the binding avidity of the constructs in comparison with native fluorescently labeled anti-CD3 antibody (Figure 2, B). Because avidity increases with increased valency of binding, and because the PEG-PAMAM constructs have a higher valence (>26 binding sites) than antibodies (2 binding sites), more of the anti-CD3 complexes bound as compared with the native antibody at a fixed ligand concentration. The concentration at which 50% of the constructs were bound was 10-fold lower than

antibody alone. Our multivalent constructs therefore allow for T-cell binding at lower concentrations of the reagent.

To test the effectiveness of this general approach in targeting antigen-specific T-cell populations that recognize peptides loaded in the context of specific MHC, we chose to study the 2C CD8⁺ T-cell line. This is a transgenic T-cell line known to be reactive to specific ligands. For example, 2C TCRs bind several ligands including the peptide SIYRYYYGL presented in the context of the self MHC H-2K^b (^{SIYK^b}) [21], and ^{SIYK^b} dimers and tetramers have been used to identify and track 2C T cells ex vivo [1,10,22]. We biotinylated the monomeric MHC, H-2K^b, at the N terminus and exogenously loaded the MHC with the SIY peptide followed by conjugation to the SA-PEG-PAMAM construct. We found that the ^{SIYK^b} constructs bound purified CD8⁺ 2C T cells with enhanced avidity as compared with ^{SIYK^b} dimers (Figure 2, C). The concentration of half-maximal binding for the multivalent constructs was 100-fold lower than dimeric forms of the MHC (^{SIYK^b}-Ig). Because the affinity of peptide-MHC–T cell interactions is much lower (1–10 μM) than antigen-antibody interactions (1–100 nM), we expected this

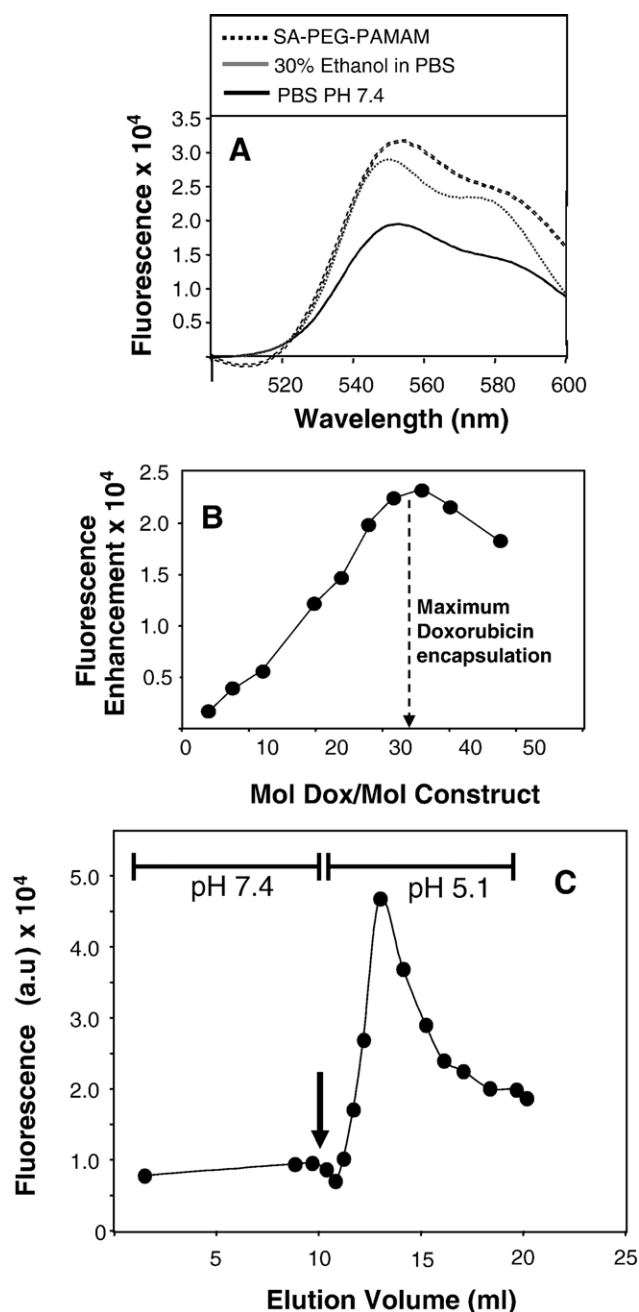


Fig 3. Doxorubicin (Dox) is efficiently encapsulated in PEG-PAMAM constructs and released at low pH. **A**, Dox fluorescence is enhanced in hydrophobic media. Emission spectra with excitation at 470 nm of Dox in PBS, in 30% ethanol-PBS, and in the presence of a 13.5 nM concentration of SA-PEG-PAMAM. **B**, Dox was titrated into a 1 mg/mL solution of SA-PEG-PAMAM, and emission spectra were collected in PBS in the presence and absence of SA-PEG-PAMAM. Fluorescence enhancement was calculated by subtracting the native Dox emission peak at 552 nm in PBS from peaks obtained in the presence of SA-PEG-PAMAM. **C**, SA-PEG-PAMAM(Dox) was dialyzed in PBS and immobilized in a 1-mL biotin-agarose column, then washed with 10 mL PBS before elution with a 10 mM acetate buffer pH 5.0. The arrow indicates beginning of elution with the acetate buffer.

enhancement in avidity to be more pronounced with constructs displaying peptide-MHC complexes.

Entrapment of Dox in the PAMAM dendritic core of antigen-presenting constructs

We hypothesized that the enhanced avidity of engineered complexes (Figure 2, B and C) when coupled with the capability to carry drugs might prove a means of drug delivery to peptide-specific T-cell populations. To test this hypothesis we first assessed the ability of our constructs to encapsulate the antimetabolic drug Dox. Previous work has shown that Dox, an anthracycline that intercalates into DNA, can exhibit antiproliferative effects and induce growth arrest and apoptosis in proliferating T cells [4]. Dox is intrinsically fluorescent, with excitation at 488 nm and peak emission at 570 nm in aqueous solutions. Dox is also a weakly basic drug (pKa = 7.6), with limited solubility in aqueous environments, partitioning more effectively into hydrophobic microenvironments. Because PAMAM constitutes the largest hydrophobic fraction of the complex, we examined the capacity of the constructs for passive loading of Dox. For these experiments we used constructs that were not conjugated with PEG-fluorescein. These unlabeled constructs were incubated with a 10-fold molar excess of Dox at 4°C for 24 hours followed by extensive dialysis. We noted a fluorescence enhancement of the encapsulated Dox after purification consistent with its preferential partitioning into the hydrophobic PAMAM core (Figure 3, A): Dox fluorescence is enhanced upon exposure to organic-aqueous media, and a similar enhancement was simulated with a 30:70 mixture of ethanol/water (Figure 3, A). Our data indicated a preferential association of Dox with SA-PEG-PAMAM similar to associations in organic-aqueous media. This association can be with the PAMAM core, through hydrophobic interactions or possibly through a combination of hydrophobic and electrostatic interactions with the immobilized streptavidin. The observed fluorescence enhancement was used to deduce the number of moles of associated drug per mole of construct (Figure 3, B). We estimated that at least 30 molecules of Dox associated with each SA-PEG-PAMAM construct (SA-PEG-PAMAM(Dox)).

Dox is efficiently released from the dendritic core at low pH

Because SA-PEG-PAMAM drug-loaded constructs are small (<100 nm), we speculated they would be efficiently internalized by target cells and become exposed to low-pH environments characteristic of lysosomal vesicles. To determine the fate of encapsulated drug upon exposure to this low-pH environment, we immobilized SA-PEG-PAMAM(Dox) in a biotinylated agarose column, and washed the column with buffered saline at pH 7.4 before addition of a low-pH buffer. Upon lowering the pH of the column to pH 5, we noted an increase in Dox concentration in the eluent as monitored by the red fluorescence of the drug (Figure 3, C). This reduction in pH is not strong

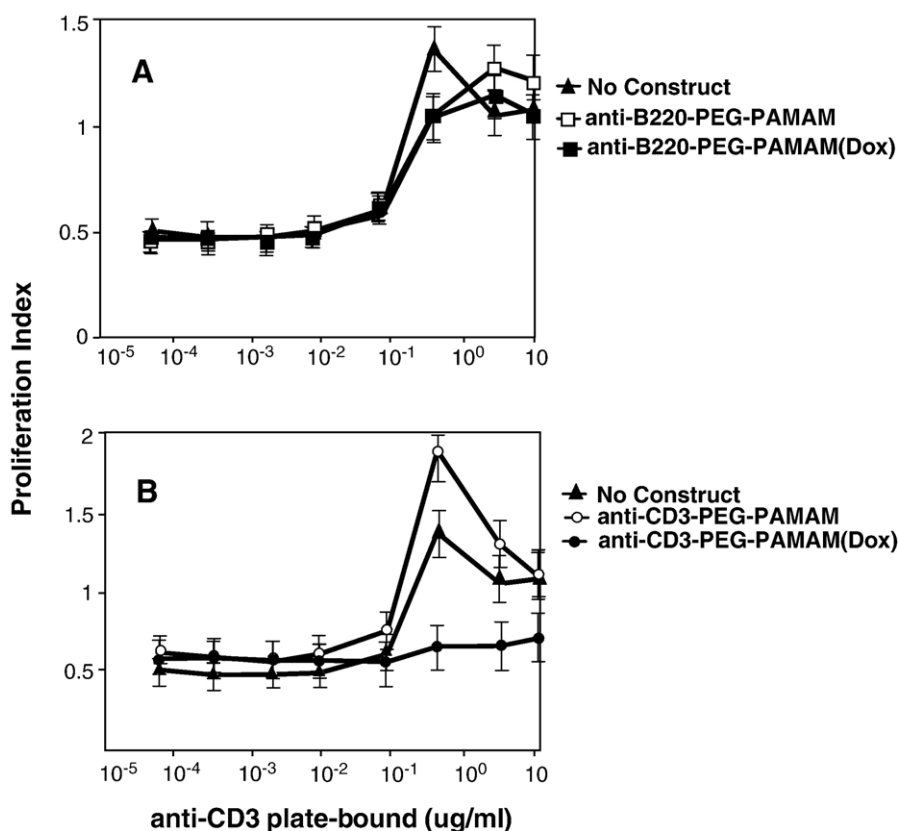


Fig 4. Inhibition of polyclonal T-cell proliferation. Unpurified murine BALB/c splenocytes (2×10^5) were stimulated by varying doses of plate-bound anti-CD3 in the presence of ($0.1 \mu\text{g/mL}$) drug-loaded or drug-free anti-B220-SA-PEG-PAMAM (A) or anti-CD3-SA-PEG-PAMAM (B). Total amount of drug offered was constant at $18 \text{ ng Dox}/\mu\text{g}$ of construct. Splenocytes were stimulated for 3 days under culture conditions and then analyzed for T-cell proliferation and viability. Proliferation index is a measure of absorbance of the colorimetric probe, WST-1 (see Methods section), which reports on proliferation and viability of cells. Error bars are the standard deviation of the mean of triplicate experiments.

enough or sufficient for the disruption of the streptavidin-biotin bond (denaturing buffers such as 8 M urea or 6 M guanidium HCl are often needed to break this bond), thus the eluent was primarily free Dox. A mass balance revealed that greater than 90% of the Dox was released from the constructs. The partitioning of Dox from a hydrophobic phase to a low-pH aqueous phase is consistent with a phenomenon described by the “ion trapping hypothesis” [23,24], wherein weak bases with a hydrophobic character such as Dox become increasingly charged with lower pH and preferentially partition to acidic compartments. Because of the small size of these complexes, they are very likely to be internalized [8,17] upon binding to target T cells and subsequently entering a low-pH lysosomal vesicle compartment in the cell—thus facilitating the pharmacological activity of the drug.

Selective inhibition of T-cell proliferation in culture

To test the biological activity of SA-PEG-PAMAM(Dox) constructs, we examined both polyclonal and antigen-specific T cells. For inhibition of proliferation of polyclonal T cells (all T cells), we stimulated unpurified splenocytes (T cells, B cells, macrophages, and a variety of other cell types) from a BALB/c mouse with varying concentrations of plate-

bound anti-CD3 ϵ in the presence and absence of Dox-loaded anti-CD3 ϵ constructs (anti-CD3-Dox) that target all T cells and Dox-loaded anti-B220 constructs (anti-B220-Dox) (a negative control that targets B cells). Compared with anti-B220-Dox, which showed little or no effect on proliferating T cells (Figure 4, A); anti-CD3-Dox inhibited their proliferation (Figure 4, B). In these experiments proliferation was affected by two competing mechanisms: an enhancement in proliferation due to the additional stimulus provided by the presentation of the anti-CD3 constructs in the medium (Figure 4, B; compare open circles to closed triangles) and an inhibition in proliferation due to specific drug delivery to target T cells (Figure 4, B; compare open circles to the other symbols). The inhibitory pharmacological Dox effect dominated over the stimulatory effect of the anti-CD3 itself.

We next investigated the efficacy of these constructs in specifically inhibiting the proliferative response of the antigen-specific 2C T-cell line. For this we chose a maximal stimulation at $1 \mu\text{g/mL}$ of anti-CD3 and incubated purified 2C CD8⁺ T cells with 2C-specific ^{SIY}K^b constructs loaded with Dox (^{SIY}K^b-Dox), a nonspecific negative control (^{SIIN}K^b-Dox), and equivalent doses of free drug. T cells were stimulated for 3 days in culture in anti-CD3 coated

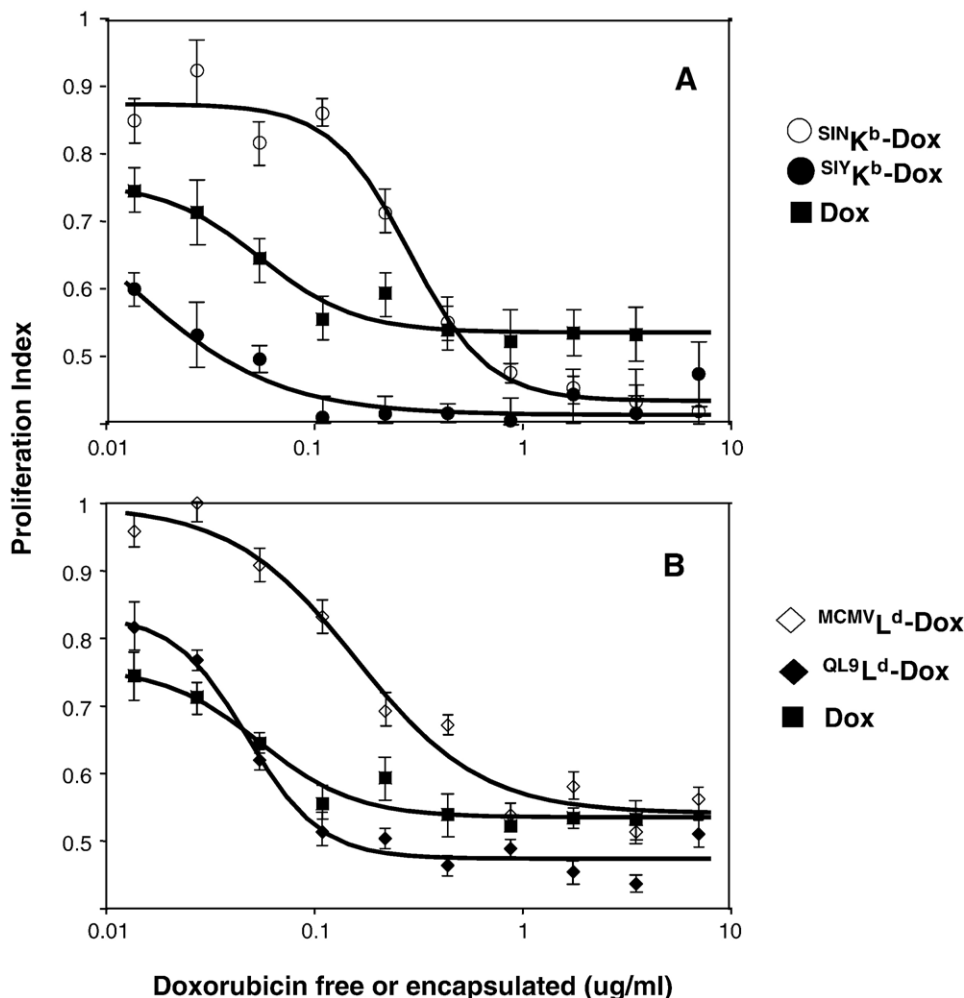


Fig 5. Inhibition of antigen-specific 2C T-cell proliferation: **A**, Purified CD8⁺ T-cell lymphocytes from 2C transgenic mice were stimulated with a fixed dose of 1 µg/mL anti-CD3 and incubated with titrated concentrations of either Dox-loaded ^{SIY}K^b-Dox or ^{SIIN}K^b-Dox, or free Dox. **B**, Incubation with either Dox-loaded ^{QL9}L^d-Dox or ^{MCMV}L^d-Dox, or free Dox. Drug loading in these constructs was estimated at 18 ng Dox/µg of construct. Proliferation was assessed 3 days after stimulation using a colorimetric assay. Error bars are the standard deviation of the mean of triplicate experiments. Curve fits are to a logistic dose-response function (see Table 1).

Table 1
Inhibition of proliferation by peptide/MHC-DOX constructs

| | Target | A ₁ ^a | A ₂ | X ₅₀ (ug/ml) | P |
|------------|--------------|-----------------------------|----------------|-------------------------|------------|
| SIYKb-DOX | Specific | 0.62 ± 0.1 | 0.42 ± 0.01 | 0.013 ± 0.02 | 2.31 ± 1.8 |
| SIINKb-DOX | Non-Specific | 0.87 ± 0.02 | 0.43 ± 0.02 | 0.29 ± 0.04 | 2.31 ± 0.6 |
| QL9Ld-DOX | Specific | 0.97 ± 0.5 | 0.47 ± 0.01 | 0.034 ± 0.04 | 1.85 ± 1.2 |
| MCMVLd-DOX | Non-Specific | 1.0 ± 0.04 | 0.54 ± 0.02 | 0.16 ± 0.04 | 1.4 ± 0.45 |
| DOX | Free Drug | 0.78 ± 0.06 | 0.53 ± 0.01 | 0.055 ± 0.02 | 1.67 ± 0.8 |

^a Values shown are derived from data fits to a logistic dose-response function (See methods). Indicated errors are standard errors calculated based on the model fit.

plates in the presence of different concentrations of specific, nonspecific, and free drug (Figure 5, A). In all cases, ^{SIY}K^b-Dox, ^{SIIN}K^b-Dox, and free Dox displayed a dose-dependent antiproliferative effect. However, ^{SIY}K^b-Dox constructs were approximately 20 times more effective in down-regulating the proliferation of 2C T cells in comparison with the nonspecific ^{SIIN}K^b-Dox. Half-maximal proliferation was achieved with 0.013 (µg/mL) of ^{SIY}K^b-Dox versus 0.29 (µg/mL) with ^{SIIN}K^b-Dox and 0.055 (µg/mL) with free Dox alone (Table 1).

To test the generality of this antigen-specific Dox inhibition, we used another peptide-MHC complex recognized by the 2C TCR with affinities similar to those of the ^{SIY}K^b complex. The 2C TCR recognizes the peptide QL9 (QLSPFPFDL) when it is presented by a foreign-derived MHC called H-2L^d, whereas the peptide MCMV (YPHFMPPTNL) is nonspecific to this system and binds the 2C TCR with extremely low affinities [25]. We observed similar results with the ^{QL9}L^d-Dox in comparison with ^{MCMV}L^d-Dox and free drug (Figure 5, B). Half-maximal

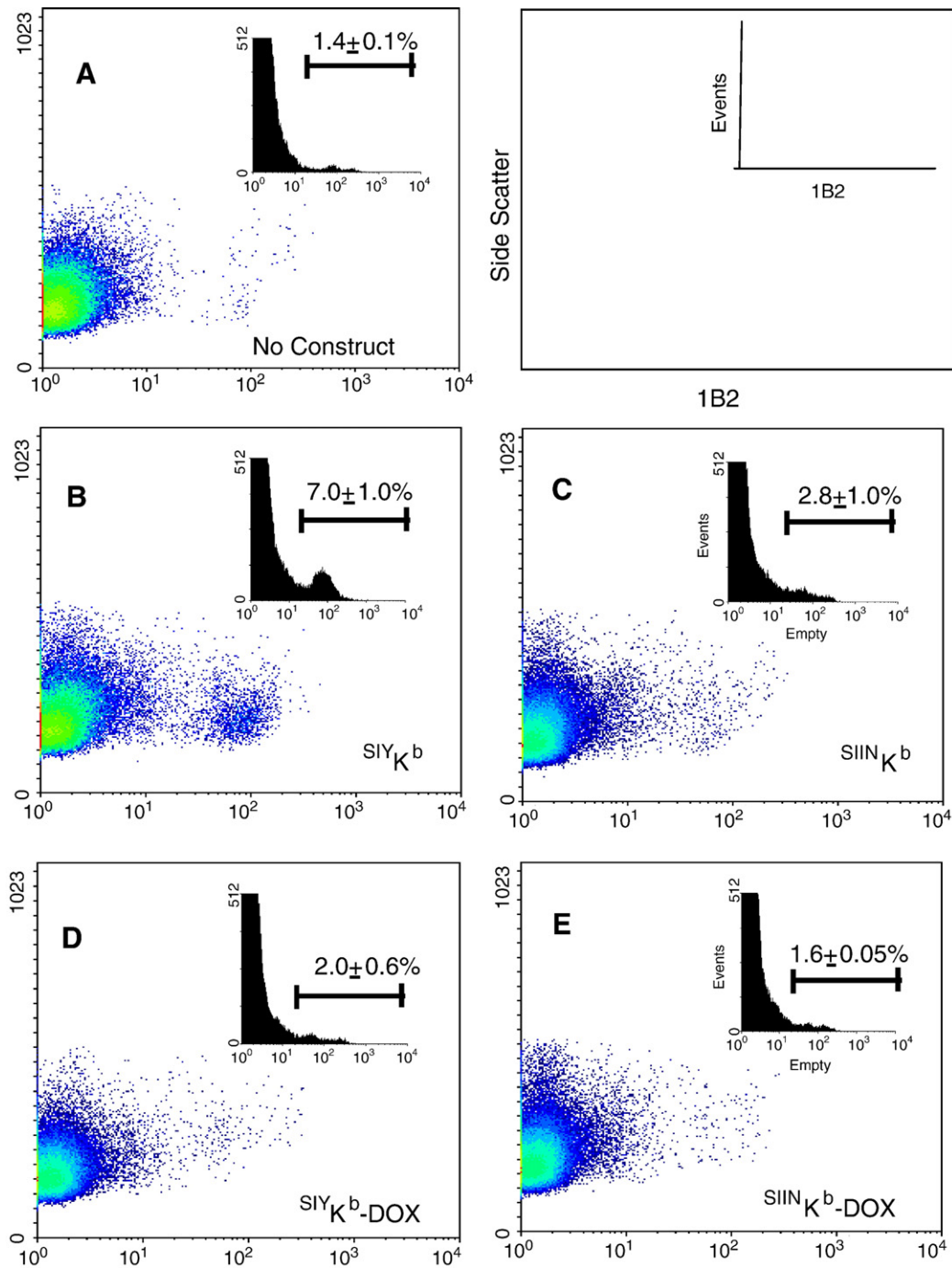


Fig 6. In vivo expansion and inhibition of adoptively transferred 2C T cells. (A) Purified CD8⁺ T cells (1×10^7) cells were adoptively transferred into age- and sex-matched naive C57BL/6 mice ($n = 4$) by tail vein injection. One day after the injection mice were challenged by intraperitoneal administration of 200 μ L of (B) $^{SIY}K^b$ construct (1 mg/mL), (C) $^{SIY}K^b$ -Dox (1.8 μ g of Dox), (D) $^{SIIN}K^b$ (1 mg/mL), (E) $^{SIIN}K^b$ -Dox (3.6 μ g of Dox). After 4 days mice were killed. Spleens were dissected and the percentage of cells that were 2C⁺ was assessed by staining with monoclonal antibody 1B2-FITC.

proliferation was achieved with 0.034 (μ g/mL) of $^{QL9}L^d$ -Dox versus 0.16 (μ g/mL) with $^{MCMV}L^d$ -Dox (Table 1).

In both the K^b and L^d cases, the drug-loaded nonspecific constructs, $^{SIIN}K^b$ -Dox and $^{MCMV}L^d$ -Dox, seemed to sequester the drug at low concentrations as compared with free drug, effectively blocking its antiproliferative activity.

The lower effectiveness of the L^d construct than the K^b construct at lower concentrations might be a result of 2C cells reacting to foreign MHC reactivity, the L^d complex. L^d is a foreign MHC to the 2C T cell, unlike K^b , which is self to the 2C T-cell transgenic mouse. This imparts additional reactivity in addition to the peptide, leading to an enhanced

stimulatory effect on 2C cells. This additional stimulatory effect might have prevailed at lower concentrations of the drug. However, for drug doses in the range of 0.1 to 10 $\mu\text{g/mL}$, both MHC constructs were clearly more effective when bound to specific peptides and exhibited enhanced toxicity to the 2C T-cell population as compared with free drug; half-maximal proliferation was fourfold higher for $\text{S}^{\text{IY}}\text{K}^{\text{b}}$ -Dox and twofold higher for $\text{Q}^{\text{L9}}\text{L}^{\text{d}}$ -dox than free drug alone (Table 1).

In vivo effects on target T-cell populations

To test for targeting and modulation of T-cell populations *in vivo*, we used a T-cell adoptive transfer procedure. In this procedure, wild-type B6 mice were injected with transgenic T cells, 1×10^7 2C CD8^+ T cells. The TCRs on those cells bind specifically to a fluorescently labeled antibody, 1B2, facilitating a method that can be used to monitor the expansion or contraction of the transgenic cells.

Mice were next challenged with drug-free $\text{S}^{\text{IY}}\text{K}^{\text{b}}$ or the nonspecific construct $\text{S}^{\text{HN}}\text{K}^{\text{b}}$ constructs. Our constructs proved to be promising stimulators for antigen-specific T cells *in vivo*. Four days after administration of the complexes, $7\% \pm 1\%$ of antigen-specific T cells responded with $\text{S}^{\text{IY}}\text{K}^{\text{b}}$ construct and ($2.8\% \pm 1\%$) with $\text{S}^{\text{HN}}\text{K}^{\text{b}}$ constructs (Figure 6, A and B). When mice were challenged with constructs loaded with Dox after adoptive transfer, this stimulatory effect was abrogated, with only $2\% \pm 0.6\%$ of the 2C population proliferating after treatment with $\text{S}^{\text{IY}}\text{K}^{\text{b}}$ -Dox (Figure 6, D). This result was consistent with our *in vitro* studies, which showed that similar doses of $\text{S}^{\text{IY}}\text{K}^{\text{b}}$ -Dox are pharmacologically more prevalent over the stimulatory effect of the $\text{S}^{\text{IY}}\text{K}^{\text{b}}$ itself and demonstrated the applicability of this system in both expansion and inhibition of antigen-specific T cells *in vivo*.

Discussion

The construct presented here is a flexible multivalent system that could be used with a variety of antibodies and peptide-MHC complexes for binding to target T cells. We have demonstrated that the resulting constructs bind with high sensitivity without loss of specificity *in vitro* and *in vivo*. This feature has obvious usefulness in high-sensitivity tracking of different types of T cells and antigen-specific T cells during normal or pathogenic immune responses [1,9,22,26]. However, our goal in this study was focused on the design of a multifunctional system, which can facilitate enhanced delivery of drugs to specific populations of T cells. Because of the functionality and demonstrated potential of PAMAM dendrimers as nanoscopic polymers in drug delivery [13], we chose these polymers as the foundation for the design of multifunctional antigen-presenting constructs. We tethered PEG to the dendrimer core for two reasons. First, PEG is a linear polymer that imparts flexibility to proteins attached to the construct and

allows for attached proteins to scan a few nanometers of surface area for attachment to cell surface receptors (see Supplementary Material section, which can be found in the online version of this article). In a multivalent system, when MHC molecules are less than 20 nm apart, T cells bind and respond more efficiently [27]. Second, proteins attached to PEG often acquire useful properties such as enhanced solubility, biocompatibility, lower immunogenicity, and desirable pharmacokinetics, while the main biological functions such as receptor recognition can often be maintained [28–30]. These are critical properties for use of this technology in *in vivo* settings.

To accommodate the attachment of a wide variety of ligands both expensive and difficult to prepare, we chose to attach streptavidin to the PEG chains as an intermediate coupling protein. Streptavidin facilitates the coupling of smaller amounts of biotinylated reagent and expands the application of the construct to a wide range of targets. In this report we demonstrated this range of usage with biotinylated reagents that target whole T-cell populations or antigen-specific T-cell populations. The intrinsic multivalent property of these reagents is especially critical for sensitive detection and drug delivery to antigen-specific T-cell populations. Increasing the affinity of weak interactions involving peptide-MHC and the TCR by multivalency facilitates slower dissociation rates and enhanced drug delivery. Although the antigen-specific T-cell studies in this report have been performed with different class I MHC proteins, the system described could be used with any biotinylated MHC applicable to other model systems without the need for complex drug conjugation chemistries and the risk of altering protein function. This additionally expands the range of use of these important proteins for both enhanced detection and modulation of antigen-specific T cells.

Furthermore, unlike protein-based delivery systems that must be prepared *de novo* and that have a limited capacity for carrying drug, the SA-PEG-PAMAM complexes described here have the capacity to carry drug, up to 32 mol of Dox per mole of construct; additionally, their utility in encapsulating a variety of low-molecular-weight drugs is documented [12]. A striking feature of this system is its ability to retard the release of the Dox drug load, effectively blocking its antimetabolic activity when the constructs are addressed with nonspecific peptide-MHC complexes. Thus, this system offers a therapeutic potential at lower concentrations comparable to dose-dense drug treatments. Additionally, they offer a distinct advantage of achieving selective expansion of T cells *in vitro* and *in vivo*, a potentially important application for cancer immunotherapy.

Acknowledgments

The authors thank Dr. Alfred Bothwell, Dr. Fadi Lakkis, and Dr. Joe Craft for helpful discussions. They also thank Dr.

Kraig Haverstick for early advice on PEG-PAMAM construction. This work was supported by grants from the National Institutes of Health (EB00487 and CA52857) and a career award to TMF from the Wallace Coulter Foundation.

References

- [1] Klenerman P, Cerundolo V, Dunbar PR. Tracking T cells with tetramers: new tales from new tools. *Nat Rev Immunol* 2002;2(4):263–72.
- [2] Howard MC, Spack EG, Choudhury K, Greten TF, Schneck JP. MHC-based diagnostics and therapeutics—clinical applications for disease-linked genes. *Immunol Today* 1999;20(4):161–5.
- [3] Schwartz RH. T cell anergy. *Annu Rev Immunol* 2003;21:305–34.
- [4] Casares S, Stan AC, Bona CA, Brumeau TD. Antigen-specific downregulation of T cells by doxorubicin delivered through a recombinant MHC II-peptide chimera. *Nat Biotechnol* 2001;19(2):142–7.
- [5] Garcia KC, Tallquist MD, Pease LR, Brunmark A, Scott CA, Degano M, et al. $\alpha\beta$ T cell receptor interactions with syngeneic and allogeneic ligands: affinity measurements and crystallization. *Proc Natl Acad Sci U S A* 1997;94(25):13838–43.
- [6] Fremont DH, Rees WA, Kozono H. Biophysical studies of T-cell receptors and their ligands. *Curr Opin Immunol* 1996;8(1):93–100.
- [7] Fahmy TM, Bieler JG, Schneck JP. Probing T cell membrane organization using dimeric MHC-Ig complexes. *J Immunol Methods* 2002;268(1):93–106.
- [8] Luo D, Haverstick K, Belcheva N, Han E, Saltzman WM. Poly(ethylene glycol)-conjugated PAMAM dendrimer for biocompatible, high-efficiency DNA delivery. *Macromolecules* 2002;35(9):3456–62.
- [9] Schneck JP. Monitoring antigen-specific T cells using MHC-Ig dimers. *Immunol Invest* 2000;29(2):163–9.
- [10] Schneck JP, Slansky JE, Herrin SMO, Greten TF. Monitoring antigen-specific T cells using MHC-Ig dimers. *New York: Wiley*; 2000. p. 17.2.1–17.2.17.
- [11] Kruisbeek AM, Shevach EM. In vitro assays for mouse lymphocyte function. *Current protocols in immunology*. New York: Wiley; 2004 [Section III: Assays for T cell Function], pp 3.12-1–3.12.20.
- [12] Esfand R, Tomalia DA. Poly(amidoamine) (PAMAM) dendrimers: from biomimicry to drug delivery and biomedical applications. *Drug Discov Today* 2001;6(8):427–36.
- [13] D'Emanuele A, Attwood D. Dendrimer-drug interactions. *Adv Drug Deliv Rev* 2005;57(15):2147–62.
- [14] Jansen JFGA, de Brabander-van den Berg EM, Meijer EW. Encapsulation of guest molecules into a dendritic box. *Science* 1994;266(5188):1226–9.
- [15] Jansen JFGA, Meijer EW, de Brabander-van den Berg EMM. The dendritic box—shape-selective liberation of encapsulated guests. *J Am Chem Soc* 1995;117(15):4417–8.
- [16] Kobayashi H, Brechbiel MW. Dendrimer-based macromolecular MRI contrast agents: characteristics and application. *Mol Imaging* 2003;2(1):1–10.
- [17] Dennig J, Duncan E. Gene transfer into eukaryotic cells using activated polyamidoamine dendrimers. *J Biotechnol* 2002;90(3-4):339–47.
- [18] Yoo H, Sazani P, Juliano RL. PAMAM dendrimers as delivery agents for antisense oligonucleotides. *Pharm Res* 1999;16(12):1799–804.
- [19] Kobayashi H, Wu C, Kim MK, Paik CH, Carrasquillo JA, Brechbiel MW. Evaluation of the in vivo biodistribution of indium-111 and yttrium-88 labeled dendrimer-1B4M-DTPA and its conjugation with anti-Tac monoclonal antibody. *Bioconjug Chem* 1999;10(1):103–11.
- [20] Tomalia DA, Naylor AM, Goddard WA. Starburst dendrimers—molecular-level control of size, shape, surface-chemistry, topology, and flexibility from atoms to macroscopic matter. *Angew Chem Int Ed Engl* 1990;29(2):138–75.
- [21] Sykulev Y, Brunmark A, Tsomides TJ, Kageyama S, Jackson M, Peterson PA. High-affinity reactions between antigen-specific T-cell receptors and peptides associated with allogeneic and syngeneic major histocompatibility complex class I proteins. *Proc Natl Acad Sci U S A* 1994;91(24):11487–91.
- [22] Dunbar PR, Ogg GS. Oligomeric MHC molecules and their homologues: state of the art. *J Immunol Methods* 2002;268(1):3–7.
- [23] Gerweck LE, Kozin SV, Stocks SJ. The pH partition theory predicts the accumulation and toxicity of doxorubicin in normal and low-pH-adapted cells. *Br J Cancer* 1999;79(5-6):838–42.
- [24] Roos A. Weak acids, weak bases, and intracellular pH. *Respir Physiol* 1978;33:27–30.
- [25] Sykulev Y, Vugmeyster Y, Brunmark A, Ploegh HL, Eisen HN. Peptide antagonism and T cell receptor interactions with peptide-MHC complexes. *Immunity* 1998;9(4):475–83.
- [26] Altman JD, Moss PA, Goulder PJ, Barouch DH, McHeyzer-Williams MG, Bell JI, et al. Phenotypic analysis of antigen-specific T lymphocytes. *Science* 1996;274(5284):94–6.
- [27] Bromley SK, Burack WR, Johnson KG, Somersalo K, Sims TN, Sumen C, et al. The immunological synapse. *Annu Rev Immunol* 2001;19:375–96.
- [28] Belcheva N, Baldwin SP, Saltzman WM. Synthesis and characterization of polymer-(multi)-peptide conjugates for control of specific cell aggregation. *J Biomat Sci Polym Ed* 1998;9(3):207–26.
- [29] Belcheva N, Woodrow-Mumford K, Mahoney MJ, Saltzman WM. Synthesis and biological activity of polyethylene glycol–mouse nerve growth factor conjugate. *Bioconjug Chem* 1999;10(6):932–7.
- [30] Katre N. The conjugation of proteins with polyethylene glycol and other polymers. Altering properties of proteins to enhance their therapeutic potential. *Adv Drug Delivery Rev* 1993;10:91–114.